Structure, Vol. 10, 1371–1381, October, 2002, ©2002 Elsevier Science Ltd. All rights reserved. PII S0969-2126(02)00864-X

Studies on the Reaction Mechanism of Riboflavin Synthase: X-Ray Crystal Structure of a Complex with 6-Carboxyethyl-7-Oxo-8-Ribityllumazine

Stefan Gerhardt,[1,4] Ann-Kathrin Schott,[2] Norman Kairies,[1] Mark Cushman,[3] Boris Illarionov,[2] Wolfgang Eisenreich,[2] Adelbert Bacher,[2] Robert Huber,[1] Stefan Steinbacher,[1] and Markus Fischer[2,4]

[1]Max-Planck-Institut für Biochemie
Abteilung Strukturforschung
Am Klopferspitz 18a
D-82152 Martinsried
Germany

[2]Lehrstuhl für Organische Chemie und Biochemie
Technische Universität München
Lichtenbergstr. 4
D-85747 Garching
Germany

[3]Department of Medicinal Chemistry
and Molecular Pharmacology
Purdue University
West Lafayette, Indiana 47907

Summary

Riboflavin synthase catalyzes the disproportionation of 6,7-dimethyl-8-ribityllumazine affording riboflavin and 5-amino-6-ribitylamino-2,4(1*H*,3*H*)-pyrimidinedione. We have determined the structure of riboflavin synthase from *Schizosaccharomyces pombe* in complex with the substrate analog, 6-carboxyethyl-7-oxo-8-ribityllumazine at 2.1 Å resolution. In contrast to the homotrimeric solution state of native riboflavin synthase, we found the enzyme to be monomeric in the crystal structure. Structural comparison of the riboflavin synthases of *S. pombe* and *Escherichia coli* suggests oligomer contact sites and delineates the catalytic site for dimerization of the substrate and subsequent fragmentation of the pentacyclic intermediate. The pentacyclic substrate dimer was modeled into the proposed active site, and its stereochemical features were determined. The model suggests that the substrate molecule at the C-terminal domain donates a four-carbon unit to the substrate molecule bound at the N-terminal domain of an adjacent subunit in the oligomer.

Introduction

Riboflavin (vitamin B_2) serves as a precursor of flavocoenzymes, which have essential roles as redox cofactors in all organisms. The final step in the biosynthesis of the vitamin is catalyzed by the enzyme riboflavin synthase [1–3]. This unusual reaction involves the dismutation of 6,7-dimethyl-8-ribityllumazine (1), affording riboflavin (6) and 5-amino-6-ribitylamino-2,4(1*H*,3*H*)-pyrimidinedione (7) (Figure 1) [4–7]. A pentacyclic intermediate of the enzyme-catalyzed reaction (4, compound Q) has been described recently [8]; riboflavin synthase can convert that compound into riboflavin and the pyrimidine derivative 7 (forward reaction) as well as into 6,7-dimethyl-8-ribityllumazine (backward reaction).

Riboflavin synthases are characterized by an internal sequence repeat, which suggested that the polypeptide folds into two domains with similar folding patterns (Figure 2) [9]. This hypothesis has been confirmed by X-ray structure analysis of riboflavin synthase of *Escherichia coli* [10]. Binding studies had shown earlier that each subunit of riboflavin synthase can bind two substrate analogs [11–15].

Surprisingly, the mechanistically complex dismutation of 6,7-dimethyl-8-ribityllumazine (1) can proceed in the absence of a catalyst [6, 16–18]. Riboflavin is formed when an aqueous solution of the lumazine derivative is boiled under reflux at neutral or acidic pH. The enzyme-catalyzed and uncatalyzed reactions proceed with identical regiospecificity [7, 16, 17].

Gram-negative bacteria and certain yeasts are unable to incorporate riboflavin from the environment and are therefore absolutely dependent on endogenous synthesis of the vitamin [19–22]. Riboflavin synthase is therefore a potential target for the development of anti-infective drugs. The design of specific enzyme inhibitors could benefit substantially from protein structure information.

The structure of riboflavin synthase from *Escherichia coli* has been determined by X-ray crystallography at a resolution of 2.1 Å [10], but the substrate binding determinants and local structure of the active site have not been elucidated unambiguously. This paper reports the structure of riboflavin synthase of *Schizosaccharomyces pombe* in complex with the substrate analog, 6-carboxyethyl-7-oxo-8-ribityllumazine (8; Figure 3).

Results

Quality of the Model

Riboflavin synthase from *S. pombe* was crystallized in complex with the bound substrate analog, 6-carboxyethyl-7-oxo-8-ribityllumazine (8; Figure 3). Native diffraction data were collected to a resolution of 2.7 Å. The crystals belonged to space group $P6_1$, with one monomer in the asymmetric unit. The crystal structure in complex with 8 was solved by multiple anomalous dispersion techniques using synchrotron radiation. The structure was refined to 2.1 Å resolution with crystallographic R values of 18.5% (R_{free} = 22.0%) with good stereochemistry (Table 1).

The final model of monomeric *S. pombe* riboflavin synthase (Figure 4A) consists of 203 residues that were well defined with the exception of the last 5 residues. Most of the side chains were clearly defined by their electron density, except for some surface-exposed residues.

[4]Correspondence: gerhardt@biochem.mpg.de (S.G.), markus.fischer@ch.tum.de (M.F.)

Key words: biosynthesis of riboflavin; riboflavin synthase; X-ray structure; *Schizosaccharomyces pombe*; reaction mechanism

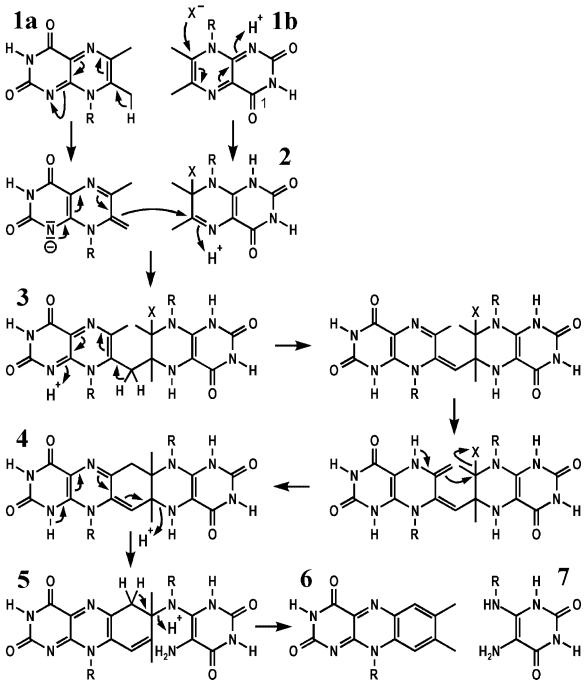

Figure 1. Hypothetical Reaction Mechanism of Riboflavin Synthase

1a, donor lumazine molecule; 1b, acceptor lumazine; X, proposed nucleophile, which neutralizes the carbonium centre at C-7 of 1b and enables carbanion attack at C-6 of 2 by the 7-exomethylene carbon of 1a [3, 30]; R, ribityl chain.

Crystal packing and the space group clearly show that the enzyme is present as a monomer in the crystals. Meanwhile, sedimentation studies had shown a trimer in solution (our unpublished data). The sedimentation equilibrium experiments were performed with a protein solution (0.7 mg/ml) containing 20 mM potassium phosphate (pH 7.0) and 100 mM potassium chloride. Notably, the trimer structure was also observed by sedimentation equilibrium analysis in the presence of the inhibitor 8, which was used in the crystallization experiments. We conclude that crystallization induces dissociation, probably as a result of the high amount of methylpentanediol present.

The temperature factors of bound 8 (23.0 Å^2) are lower than those of the protein on average (27.2 Å^2) (Table 1). Correspondingly, the two ligand molecules were well defined in the final electron density maps (Figure 5), indicating clearly the proposed active site arrangements and allowing insights into the reaction mechanism of riboflavin biosynthesis.

Structural Overview

Riboflavin synthases from *E. coli* and *B. subtilis* are both homotrimers in solution as shown by hydrodynamic studies [23, 24]. The crystal structure of the ligand-free enzyme of *E. coli* has been reported [10]. The enzyme is an asymmetric trimer with the subunits related to one another by rotations of 124°, 85°, and 151°. Trimerization occurs principally via the C-terminal helices, but does not lead to a symmetrical structure. The recombinant expression of the N-terminal domain of the *E. coli* protein afforded a c_2 symmetric homodimer [25, 26].

The monomeric *S. pombe* riboflavin synthase model consists of 203 amino acids, arranged in an N-terminal β barrel (residues 1–90), an almost identically folded C β barrel (residues 91–184), and a C-terminal α helix (residues 185–203) (Figure 4A). Superimposition of 168 α-carbon atoms including both β barrels and the C-terminal helix of the monomers of riboflavin synthase from *S. pombe* and *E. coli* reflects their high structural similarity by an rmsd value of 0.8 Å (Figure 6).

A structural comparison of the N-terminal β barrel and the C β barrel of *S. pombe* riboflavin synthase (Figure 4B) shows their internal pseudo-2-fold symmetry with an rmsd value of 0.97 Å for 84 α-carbon atoms.

Binding of a Substrate Analog Inhibitor to the β Barrel Domains

We cocrystallized riboflavin synthase from *S. pombe* with a derivative of substrate 1, 6-carboxyethyl-7-oxo-8-ribityllumazine (8). This tightly bound inhibitor molecule is well defined in its electron density map at 2.1 Å resolution and clearly indicates the location of the two substrate binding sites of each β barrel domain (Figure 5). By comparison of the two barrel domains, the positions of the bound substrate analog of each barrel are matched almost exactly (Figure 2B). The substrate analogs are mainly bound through hydrophilic side chain and main chain interactions (Figures 3A and 3B). In contrast to the binding of 6-carboxyethyl-7-oxo-8-ribityllumazine to 6,7-dimethyl-8-ribityllumazine synthase of *S. pombe* [27], the upstream enzyme in the riboflavin synthetic pathway, 8 is bound to *S. pombe* riboflavin synthase without contributions by aromatic stacking interactions.

6-Carboxyethyl-7-Oxo-8-Ribityllumazine Binding to the N-Terminal Barrel

The lumazine chromophore of 8 in the N-terminal β barrel is exclusively involved in hydrophilic interactions (Figure 3A). The strictly conserved active site residue, His102, the only aromatic residue in the N-terminal active site, forms only a hydrogen bond by its side chain to the oxo substituent at position 7 of the lumazine ring. The peptide amide groups of Ala64 and Thr50 are oriented toward the O2 and O4 carbonyl groups of the ligand lumazine ring at distances of 2.7 Å and 2.9 Å, respectively. In addition, the side chain oxygen atom of Thr50 is involved in a hydrogen-bonding interaction with the imido group N5 of the ring system. The carbonyl oxygen of Gly62 is strongly hydrogen bonded to the N3-imide hydrogen atom of the CEOL inhibitor at a distance of 2.7 Å. The side chain oxygen γ-O of Ser67 is involved in an additional hydrophilic interaction to the O2 carbonyl group and further in a hydrogen bond interaction to the OH3 hydroxyl group of the ribityl side chain of the lumazine ring system. The next ribityl hydroxyl group OH4 is hydrogen bonded to the main chain amide group of Val103. The residues Val103 and His102 take part in 8 binding from the following C barrel of the *S. pombe* riboflavin synthase monomer. The distance between the

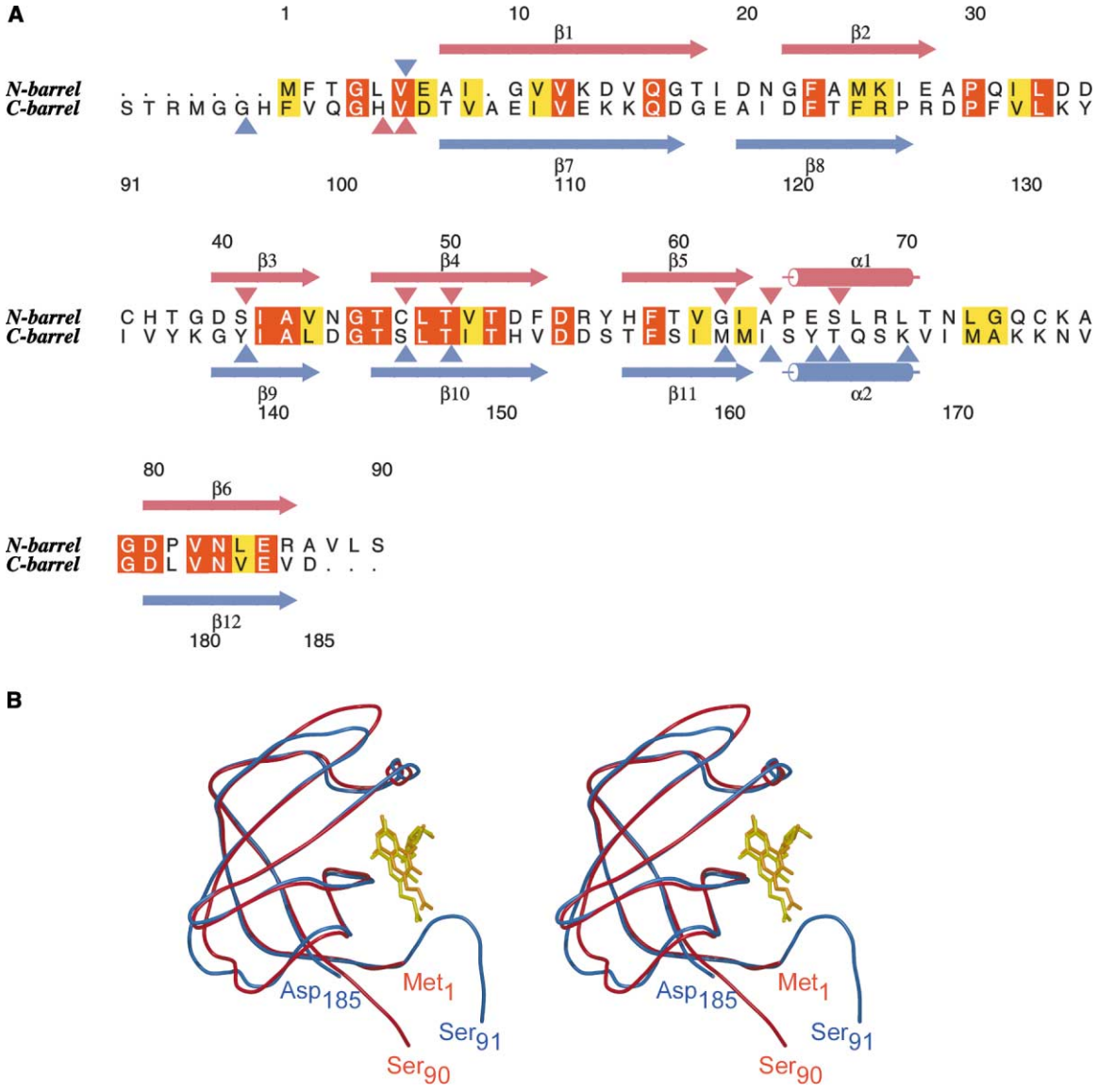

Figure 2. Internal Sequence Alignment of Riboflavin Synthase

(A) Alignment of the N barrel (red) and the C barrel (blue) domains of *S. pombe*.

(B) Stereo diagram of an internal superposition of the two β barrels with bound 6-carboxyethyl-7-oxo-8-ribityllumazine.

thiol group of Cys48 and carbon atom 6 of 8 is 4.0 Å (Figure 3C).

6-Carboxyethyl-7-Oxo-8-Ribityllumazine Binding to the C-Terminal Barrel

The binding arrangement of 8 in the C β barrel is almost the same as for the N-terminal barrel mentioned above (Figure 3B). The two aromatic residues, Tyr139 and Tyr164, interact with the bound ligand *via* hydrogen bonds to the carboxyethyl substituent at position 6 of the lumazine derivative and its ribityl side chain, respectively. The peptide amide groups of Ile162 and Thr148 are in hydrogen-bonding distance with the O2 and O4 carbonyl groups of the ligand lumazine system. The active site residue Thr148 of the C barrel is in the same topological position as the corresponding Thr50 of the N-terminal barrel and establishes identical hydrogen bonds. The carbonyl oxygen of Met160 is strongly hydrogen bonded to the N3-imide hydrogen atom of the inhibitor at a distance of 2.7 Å. Ser67 of the N-terminal barrel is replaced by the corresponding Thr165. In the C-terminal barrel, Thr165 is hydrogen bonded to the O2 carbonyl group. Corresponding to the N-terminal barrel, the OH3 hydroxyl group of the ribityl side chain of the lumazine ligand is in hydrogen-bonding distance to the γ-O atom of Thr165. Only the active site residue Val6 of the adjacent N-terminal barrel is involved with the main chain amide group in a hydrogen contact to the ribityl hydroxyl group OH4 of the bound CEOL in the C barrel of the *S. pombe* riboflavin synthase monomer. Whereas most amino acid residues in direct contact with the lumazine chromophore are identical at the N- and C-ter-

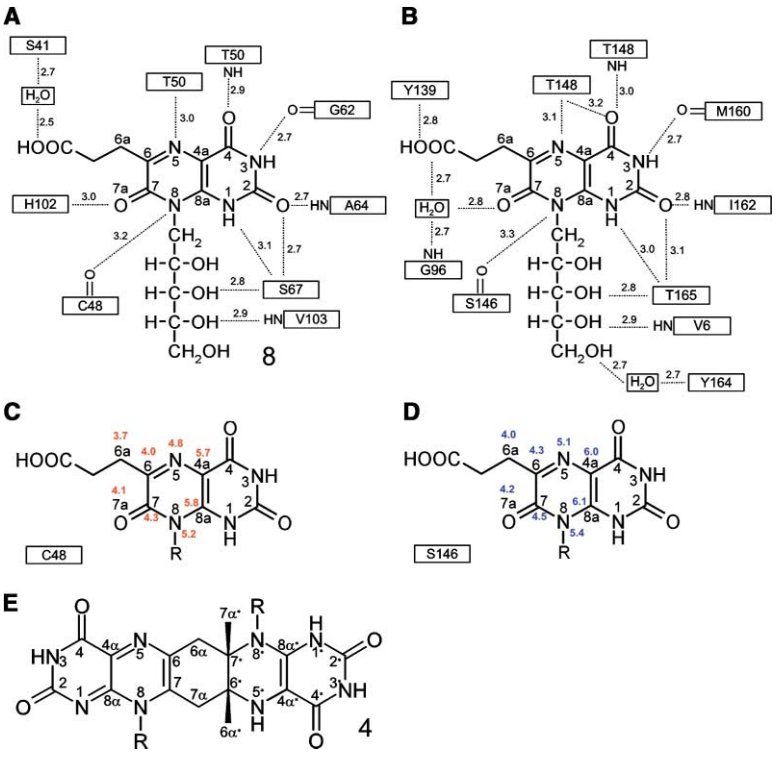

Figure 3. Hydrogen-Bonding Topology of 6-Carboxyethyl-7-Oxo-8-Ribityllumazine (8) Bound to *S. pombe* Riboflavin Synthase

N-terminal domain (A); C-terminal domain (B); distances from the thiolate group of cysteine 48 (C); distances from the side chain oxygen of serine 146 (D); compound Q (E).

minal binding sites, the amino acid topologically equivalent to cysteine 48 of the N β barrel is the serine residue 146 of the N β barrel.

Discussion

The benzenoid ring of riboflavin originates in a most unusual way by dismutation of the pteridine derivative 1. The available information on the reaction mechanism can be summarized as follows. (1) The enzyme-catalyzed reaction requires no organic cofactors and no metal ions [15]. (2) The reaction can proceed in the absence of a catalyst in neutral or acidic aqueous solution [16–18]. (3) The pentacyclic lumazine dimer 4 fulfills the criteria for a kinetically competent reaction intermediate [8]. (4) The pentacyclic intermediate can be cleaved by riboflavin synthase to yield either riboflavin (6) and the pyrimidine 7 or two molecules of the riboflavin synthase substrate 1. (5) An isotope effect of 5.0 has been found for [6α-$^2H_3$]6,7-dimethyl-8-ribityllumazine [5]. Hence, the release of a proton(s) from the position 6 methyl group could involve a relatively high energy barrier.

Riboflavin synthase of bacteria and yeasts, including *S. pombe*, are homotrimeric proteins in solution. The quaternary structure of the *S. pombe* enzyme in solution is not affected by the ligand 8, the ligand used in the present crystallographic study (our unpublished data). Hence, the monomer structure found in the crystals must be due to the crystallization buffer, most probably by the organic solvent used as precipitant.

The riboflavin synthase subunit folds into two domains with closely similar folding topology (0.97 Å rmsd in case of the *S. pombe* enzyme; Figure 2). This had been anticipated on the basis of sequence arguments [9] and has been confirmed by X-ray structure analysis of riboflavin synthase of *E. coli* (without bound ligand) [10] and of *S. pombe* (with bound ligand). In the crystals of the *S. pombe* protein, the two folding domains are related by a noncrystallographic pseudo-c_2 symmetry axis with a rotation angle of 176.2° (Figure 4B).

Both domains of the *S. pombe* protein can bind one molecule of the enzyme inhibitor, 6-carboxyethyl-7-oxo-8-ribityllumazine, in shallow cavities lined by hydrophilic groups. The conformations of the ligand molecules bound to the N- and C-terminal domains are closely similar. The amino acid residues in contact with the bound ligand are also closely similar. The major difference is a cysteine residue (position 48 in the N-terminal domain) being replaced by a serine residue (position 146 in the C-terminal domain). Both amino acids are absolutely conserved in all putative riboflavin synthase paralogs. Nevertheless, serine 146 of the *S. pombe* enzyme can be replaced by alanine with only a minor impact on enzyme activity. Replacement of cysteine 48 by serine reduces the activity by a factor of five, but replacement by alanine affords a soluble protein whose activity, if any, is below the level of detection (our unpublished data). It should also be noted that mutant genes specifying *E. coli* riboflavin synthase mutants carrying alanine or serine instead of cysteine 48 (corresponding to cysteine 48 of the *S. pombe* enzyme) could not be expressed in recombinant *E. coli* strains [28]. Distances of the side chain heteroatom of cysteine 48 and serine 146 to atoms of the bound enzyme inhibitors are shown in Figures 3C and 3D. The closest neighbor of the thiol group is the 6α-methylene group of the ligand (3.7 Å).

The folding topologies of the *E. coli* and *S. pombe* enzymes are closely similar (Figure 6). Moreover, the

Table 1. X-Ray Data Processing and Refinement Statistics

	DERI (Thiomersal)			NATI
Cell constants (Å)				
$a = b$	70.50			70.32
c	92.95			92.37
Space group	$P6_1$			$P6_1$
Resolution limit (Å)	2.1			2.7
Reflections, unique	15,097			6,988
	Remote	Peak	Edge	
Wavelength (Å)	0.94991	1.000	1.010	
Multiplicity[a]	2.0	2.0	2.0	2.7
R_{merge}[b] overall	0.097	0.098	0.101	0.127
R_{merge}[a,c]	0.265	0.302	0.314	0.348
Completeness overall (%)	94.5	94.5	93.1	97.8
Completeness (%)[c]	95.3	95.2	69.8	97.8
Reflections[a]	28,494	28,350	27,976	
Completeness anomalous (%)	89.8	89.4	89.5	
Nonhydrogen protein atoms	1,558			1,558
Solvent molecules	121			79
Nonhydrogen ligand atoms	54			54
Nonhydrogen ion atoms	1			—
Resolution range (Å)	19.88–2.1			20.6–2.7
R value overall (%)[d]	18.5			19.8
R_{free} (%)	22.0			26.3
Root mean standard deviations				
Bond lengths (Å)	0.006			0.007
Bond angles (°)	1.24			1.21
Average B values (Å^2)				
Protein	27.2			28.6
Ligand	23.0			26.9
Solvent	32.4			28.7
Ion	40.6			—
ϕ, Ψ angle distribution for residues[e]				
In most favored regions (%)	86.0			80.3
In additional allowed regions (%)	14.0			19.7
In generously allowed regions (%)	0.0			0.0
In disallowed regions (%)	0.0			0.0

[a] Friedel-Mates treated as independent reflections.
[b] $R_{merge} = \Sigma_{hkl}\,[(\Sigma_i|I_i - <I>|)/\Sigma_i I_i]$
[c] Values correspond to the highest resolution shell (Hg derivative, 2.14–2.1 Å; native, 2.85–2.7 Å).
[d] R value $= \Sigma_{hkl}\,||F_{obs}| - |F_{calc}||/\Sigma_{hkl}|F_{obs}|$
[e] Ramachandran statistics as defined by PROCHECK [43].
R_{free} is the crossvalidation R factor computed for the test set of 10% of unique reflections.

amino acids in direct contact with the bound ligand are identical or very similar in the *E. coli* enzyme (Figure 7). Therefore, the lumazine analog could be modeled easily from the *S. pombe* structure to all six binding sites of the *E. coli* enzyme (Figure 4C).

The *E. coli* riboflavin synthase is devoid of trigonal symmetry [10]. Trimerization occurs via the C-terminal helices. Only the N-terminal domain of one subunit has extended contacts with the C barrel domain of a second subunit. Only in one out of three potential active sites, two subunits are in close contact and form an active site with pseudo-c_2 symmetry (Figure 8), where the substrate molecules are ideally positioned for the dismutation reaction.

Indirect evidence for the nonsymmetrical character of riboflavin synthases had been obtained earlier by protein perturbation experiments using fluorinated pteridine derivatives which were monitored by ^{19}F NMR [12, 13, 28, 29]. Multiple ^{19}F NMR signals were observed for trifluoromethyl groups of enzyme-bound ligands, which were best explained by the hypothesis that the ligand molecules are bound in different environments. Recent NMR experiments with the *S. pombe* enzyme gave similar results (our unpublished data). We conclude that the asymmetry observed with the unliganded *E. coli* riboflavin synthase persists in the presence of ligands. The protein perturbation studies are well in line with the hypothesis of major dynamic motions in the homotrimeric protein which could bring N- and C-terminal domains of different subunits into the appropriate spatial relationship for substrate dimerization. The crystal structure of the *E. coli* enzyme would then have to be interpreted as a snapshot of a specific conformation which is stabilized by crystal contacts.

In order to analyze the reaction mechanism in closer detail, we replaced the inhibitor molecules in Figure 9A (1) by the substrate 6,7-dimethyl-8-ribityllumazine (Figure 9B) and (2) by the pentacyclic reaction intermediate 4 (Figure 9C).

The stereochemistry of the pentacyclic intermediates has not been determined hitherto. It appears plausible that the dimerization of 6,7-dimethyl-8-ribityllumazine

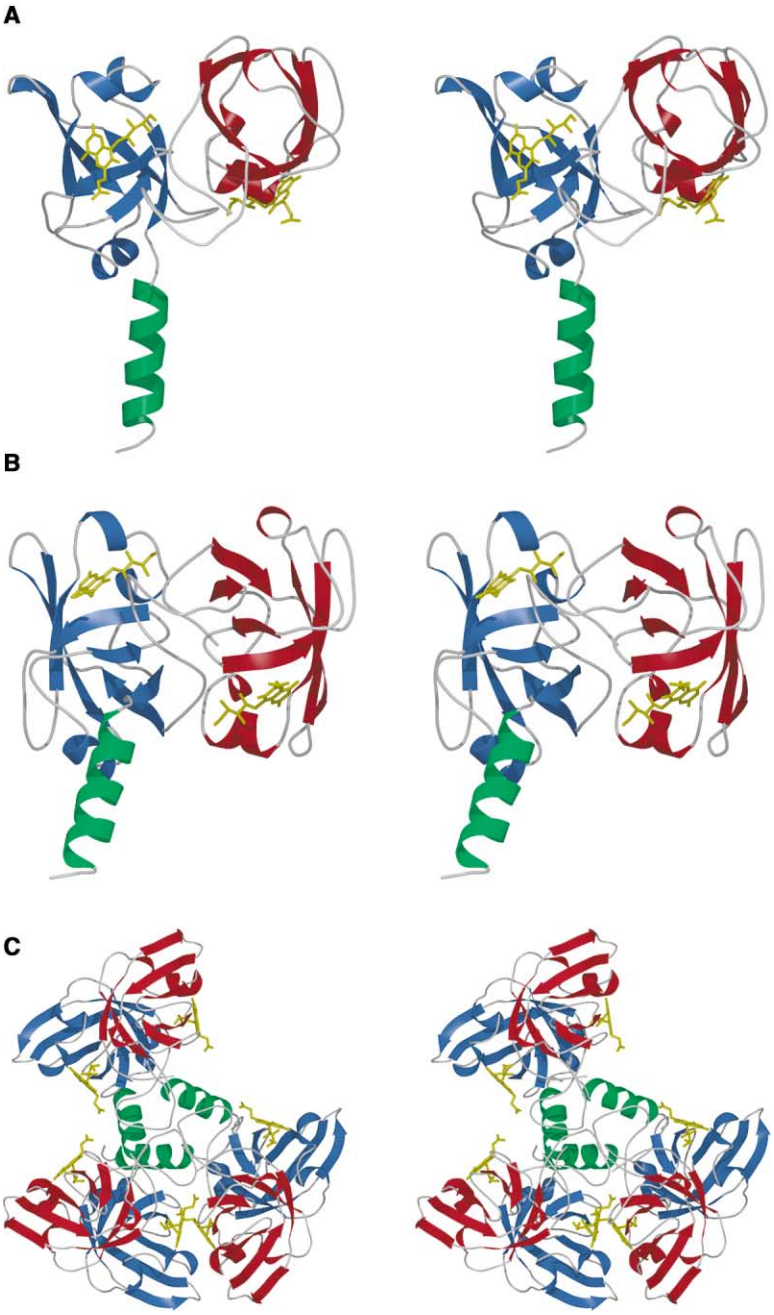

Figure 4. The *S. pombe* Riboflavin Synthase Monomer and Proposed Trimer

Stereo diagrams of the *S. pombe* riboflavin synthase monomer (A) with bound 6-carboxyethyl-7-oxo-8-ribityllumazine (yellow); a view along the pseudo-2-fold symmetry axis of the two folding domains (B); the trimeric model of *S. pombe* riboflavin synthase (C) with bound 6-carboxyethyl-7-oxo-8-ribityllumazine (yellow).

should result in *syn* linkage of the ring systems of donor molecule 1a and receptor molecule 1b (Figure 1). Of the two diastereomers (6*R;7*S) and (6*S;7*R), only (6*R;7*S) (Figure 3E) fits into the cavity formed at the interface of the N- and C-terminal domains of subunits A and C of the *E. coli* enzyme.

The result of a dynamics simulation described in Experimental Procedures is shown in Figure 9C. The pentacyclic substrate dimer fits closely into the putative active site of *S. pombe* riboflavin synthase generated with the coordinates of the *E. coli* enzyme [10]. Upon enzymatic cleavage of the dimer, the resulting riboflavin would be bound to the N-terminal domain, and the pyrimidine product would be bound to the C-terminal domain. In other words, the lumazine molecule originally bound to the N-terminal domain is the four-carbon acceptor and the substrate bound to the C-terminal domain is the four-carbon donor.

With this in mind, the thiolate group of cysteine 48 may act as a base which abstracts a proton from the 6α-methylene group in the hypothetical reaction intermediate 4 and/or 5. However, it should be noted that the catalytic activity of the enzyme is only reduced 6-fold by replacement of cysteine 48 with serine, although the K_A values of cysteine and serine differ by at least five orders of magnitude.

The serine residue 146 could act as the nucleophile X proposed by Plaut and Beach [3]. However, it is also possible that this function could be assumed by a water molecule, since the reaction can proceed without enzyme

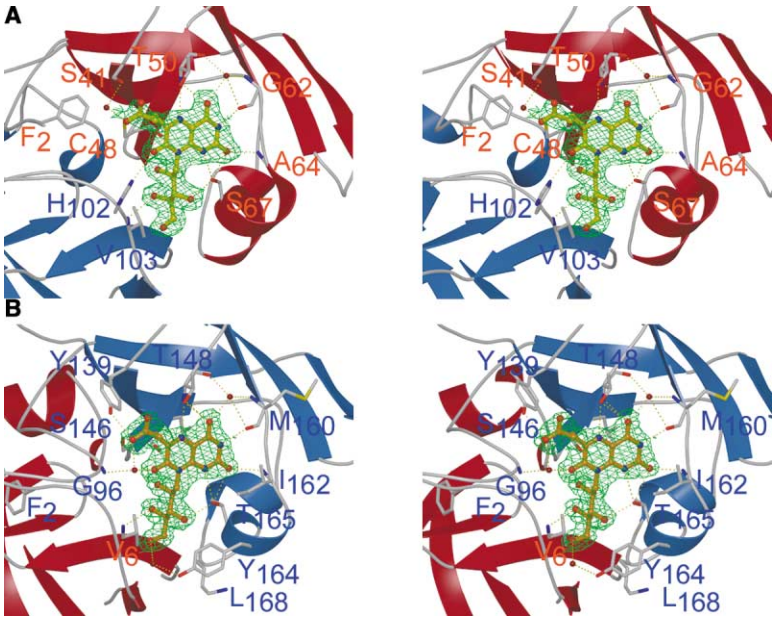

Figure 5. Stereo Views of the Substrate Binding Site of Riboflavin Synthase from *S. pombe*

Comparison of 6-carboxyethyl-7-oxo-8-ribityllumazine binding to the N barrel ([A], red) and C barrel ([B], blue). The refined $2F_o - F_c$ electron density maps covering the bound ligands are contoured at 1.0 σ.

catalysis. This would fit the observation that, although serine 146 appears to be absolutely conserved, it can be replaced with only minor impact on catalytic rate.

Plaut and Beach proposed an elegant hypothesis suggesting that the hydroxyl group of the position 8 ribityl side chain of 2 could act as a nucleophile attacking position 7 of the pteridine system under formation of a tricyclic reaction intermediate [30]. Indeed, the formation of tricyclic lumazine anion structures has been shown in solution [31–33]. The X-ray structure of the *S. pombe* enzyme shows the ribityl side chains of both substrate molecules to be bound strongly in an extended conformation. This appears inconsistent with the proposed tricyclic anion intermediate. On the contrary, the polyol side chains of both substrate molecules are likely to retain an extended conformation throughout the complex reaction trajectory.

Biological Implications

Riboflavin synthase performs an unusual dismutation reaction in which two identical substrate molecules serve as donor (1a) or acceptor (1b) of a four-carbon unit. Previous structural analysis [10] and NMR studies (our unpublished data) [9, 23, 24] revealed a markedly nonsymmetric trimeric state of riboflavin synthase. Our modeling experiments, based on the inhibitor-bound protein, strongly suggest that the close intersubunit contact of the trimer as seen in the crystals of the *E. coli* protein is indeed in an active conformation and capable of supporting the dismutation reaction. Therefore, this trimer very likely represents a distinct functional state. As there is no reason to suggest a static asymmetric ensemble, it appears likely that thermal fluctuation or substrate binding converts the three different intersubunit contacts into one another, retaining an asymmetric trimer.

We demonstrate here that the reaction is achieved by binding the substrate molecules in a pseudo-c_2 symmetric environment, where the C-terminal domain acts as donor site and the N-terminal domain as acceptor site. In addition, the geometry of the active site allows us to suggest the stereochemistry of the pentacyclic intermediate 4.

The enzymes of the riboflavin biosynthetic pathway are essential enzymes in enterobacteria or yeasts as a

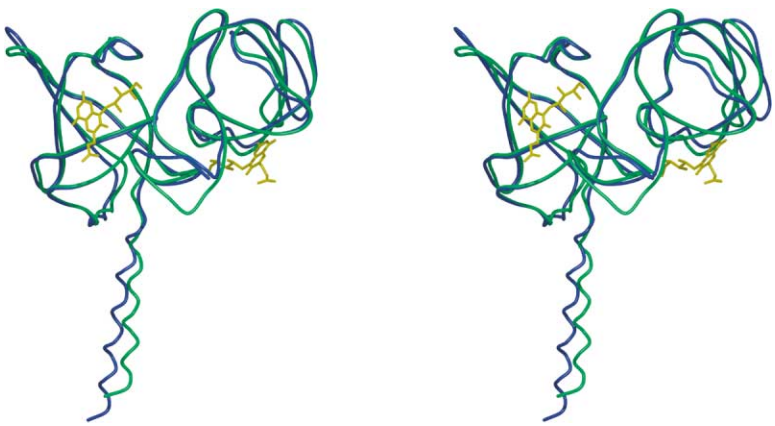

Figure 6. Structural Comparison

Stereo diagram of the superposition of one subunit of riboflavin synthase from *E. coli* (blue) and *S. pombe* (green).

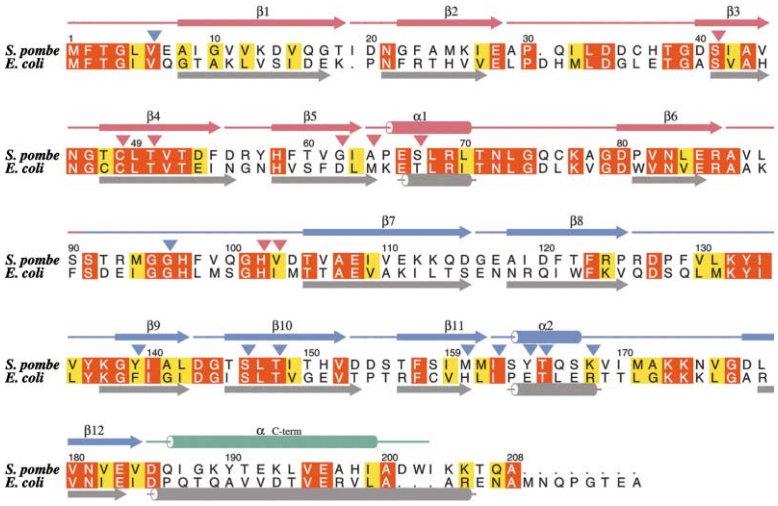

Figure 7. Structural Sequence Alignment of Riboflavin Synthase from *S. pombe* and *E. coli*

The numbering above the alignment corresponds to wild-type enzyme from *S. pombe*. Red arrows indicate the residues involved in 6-carboxyethyl-7-oxo-8-ribityllumazine binding to the N-terminal β barrel. Blue arrows indicate the residues involved in 6-carboxyethyl-7-oxo-8-ribityllumazine binding to the C-terminal β barrel of the *S. pombe* enzyme.

consequence of the apparent absence of a flavin uptake system. Therefore, riboflavin synthase itself is a potential target for anti-infective drugs. The detailed analysis of the reaction mechanism could reveal new insights for the development of mechanism-based enzyme inhibitors designed for therapeutic application. The pseudo-c_2 symmetric active site allows the design of inhibitors that link the donor and acceptor domains with a single inhibitor as a novel strategy for inhibitor design [29].

Experimental Procedures

Materials

6-Carboxyethyl-7-oxo-8-ribityllumazine was prepared by published procedures [34]. Recombinant riboflavin synthase of *S. pombe* was prepared (our unpublished data).

Crystallization

Crystals of *S. pombe* riboflavin synthase in complex with 6-carboxyethyl-7-oxo-8-ribityllumazine of maximal dimensions 0.2 mm × 0.05 mm × 0.05 mm grew within a few days by sitting drop vapor diffusion against a 0.3 ml reservoir solution containing 0.1 M bicine (pH 9.0) and 65% (v/v) 2-methyl-2,4-pentanediol (MPD). Droplets were composed of 2 μl enzyme solution (9 mg/ml of 20 mM Tris hydrochloride [pH 7.0], containing 100 mM potassium chloride and a 10 molar excess of solid 8) and 2 μl of reservoir buffer. For data collection, these cocrystals could be frozen at 100 K in reservoir buffer serving as a cryoprotectant due to its high content of MPD.

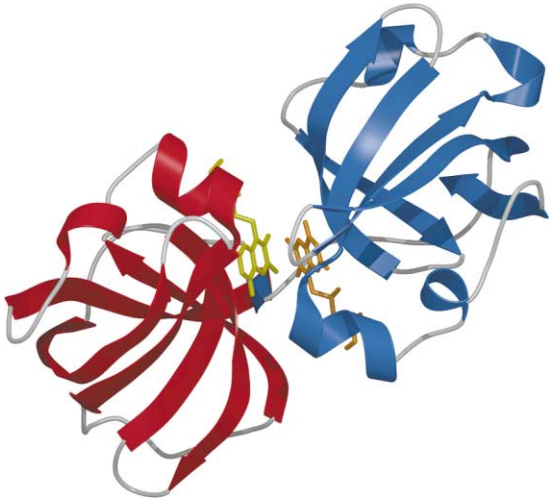

Figure 8. Proposed Active Site Dimer of *S. pombe* Riboflavin Synthase with Modeled Substrate 2

View along a pseudo-2-fold symmetry axis of the two barrel domains of adjacent subunits.

Data Collection and Structure Solution

Native X-ray data (NATI) for the inhibitor-bound wild-type enzyme were collected on a MAR Research 345 imaging plate detector system mounted on a Rigaku RU-200 rotating anode operated at 50 mA and 100 kV with $\lambda = CuK_\alpha = 1.542$ Å under cryogenic conditions. The X-ray intensities were evaluated up to 2.7 Å by using the MOSFLM [35] program package. The crystals complexed with 8 belong to the space group $P6_1$ with cell constants a = b = 70.32 Å, c = 92.37 Å. The asymmetric unit contained one monomer resulting in a Matthews coefficient of 3.0 Å^3/Da [36] with a solvent content of 59%.

Heavy atom derivatives were prepared by soaking the cocrystals at room temperature either in 2 mM thiomersal ($C_9H_9HgNaO_2S$) for 2 hr or incubation with tantalum bromide ($Ta_6Br_{12}^{2+}$) overnight. The corresponding derivatives and double derivatives were analyzed by difference Patterson methods and cross-phased difference Fourier maps with MLPHARE [37].

Anomalous data (DERI) for MAD phasing were collected from a single cross-phased characterized mercury heavy atom cocrystal at the DESY synchrotron source beamline BW6 (Hamburg, Germany) employing a MAR Research CCD detector. The derivatized cocrystal was frozen at 100 K, with the mother liquor serving as a cryoprotectant. The MAD data up to 2.1 Å were measured at Hg-K absorption edges f′ (1.010 Å) and f″ (1.000 Å) and the remote wavelength at 0.9499 Å. Complete data sets were recorded in rotation frames of 0.5° per angular range of 90° followed by a continuous set of 90° for measured Friedel pairs in inverse beam geometry. All data sets were integrated and scaled with the HKL package [38] and further processed using programs from the CCP4 suite [39]. Data collection statistics are shown in Table 1. One mercury position could be confirmed in anomalous difference Patterson maps and was used for initial phasing with MLPHARE [37]. Phases were improved by solvent flattening and density modification. The experimental MAD map had an overall figure of merit of 0.55 (Table 2) and allowed tracing of most of the polypeptide chain, including side chains.

Examination of the packing indicated reasonable crystal contacts between the riboflavin synthase monomers without overlap of symmetry-related molecules.

Model Building and Refinement

Model building was carried out with the program MAIN [40]. The initial model was subjected to rigid body and positional refinement using CNS [41]. After several cycles of manual rebuilding, positional

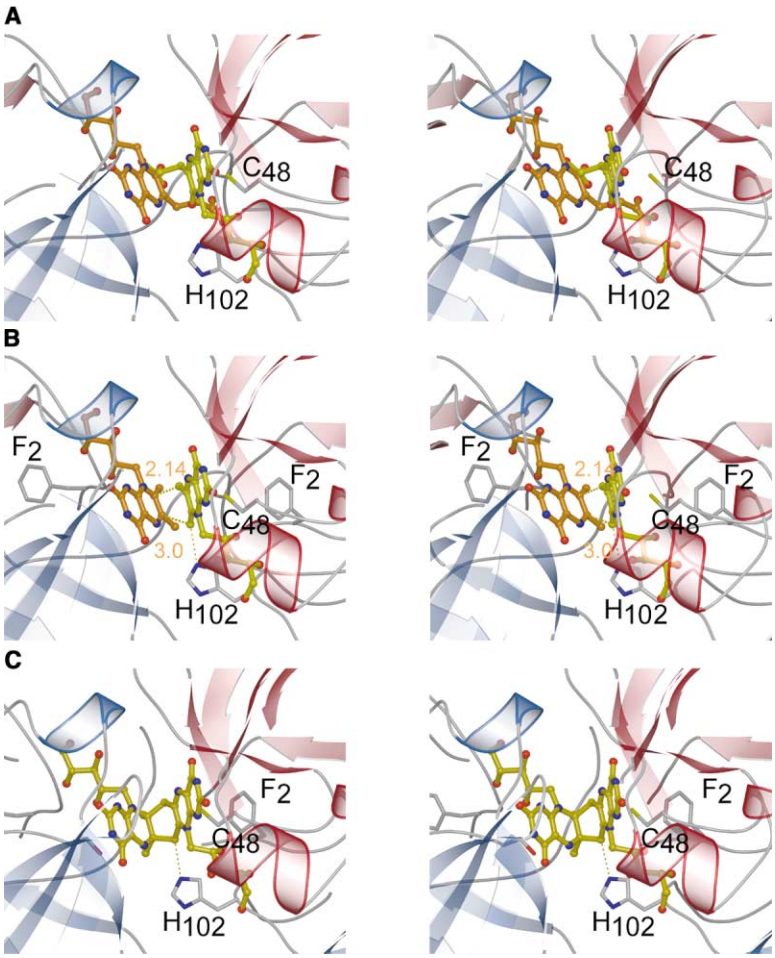

Figure 9. Studies on the Reaction Mechanism

Stereo view of the active site residues formed by two adjacent riboflavin synthase monomers of *S. pombe* with bound 6-carboxyethyl-7-oxo-8-ribityllumazine (A). The ligand bound to the N barrel (red) is drawn in yellow, whereas the 6-carboxyethyl-7-oxo-8-ribityllumazine in the adjacent C barrel (blue) is shown in dark yellow.

(B) Proposed binding of 6,7-dimethyl-8-ribityllumazine at the active site.

(C) Model for the pentacyclic reaction intermediate 4 [8].

and B factor refinement and two rounds of simulated annealing water molecules were incorporated automatically into the *S. pombe* riboflavin synthase model at 2.1 Å resolution. The progress of all refinement procedures was monitored by using 10% of the reflections to calculate a free R value (R_{free}). A geometry check using the program PROCHECK [42] revealed that 86.0% and 14.0% of all nonglycine residues lie within the most favored and additionally allowed regions of the Ramachandran plot, respectively (Table 1) [43].

Molecular Modeling

Using SYBYL modeling software [44], two substrate molecules, 6,7-dimethyl-8-ribityllumazine (1) and the reaction intermediate 4, were generated and modeled into the proposed active site formed by two adjacent *S. pombe* riboflavin synthase monomers. This active dimer was generated by superposition of *S. pombe* riboflavin synthase monomers on the crystal structure of the *E. coli* trimer (1I8D).

Correct atom types, stereocenters, hybridization states, and bond types were defined, and Gasteiger-Hückel charges were assigned to each atom. A spherical subset of 8 Å radius around compound 4 was defined and energy minimized using the Powell method and the Tripos force field. The remaining protein was treated as rigid body during energy minimization.

Analysis and Graphical Representation

Stereochemical parameters were assessed with PROCHECK [42]. Protein structures were aligned three-dimensionally by TOP3D [39], and

Table 2. MAD Data Statistics for the Hg Derivative (Thiomersal, DERI)

Figure of merit (FOM)	0.55		
	Remote	Peak	Edge
Wavelength (Å)	0.94991	1.000	1.010
Phasing power			
Iso (centric)	—	1.23 (34)	0.72 (318)
Ano (acentric)	—	0.89 (8499)	0.99 (8533)
R_{Cullis}[a]			
Iso (centric)	—	0.79 (311)	0.85 (318)
Iso (acentric)	—	0.79 (8499)	0.83 (8533)
Ano	0.84 (8427)	0.75 (8399)	0.73 (8394)

[a] $R_{Cullis} = \Sigma_{hkl}||F_{PH}(hkl)| \pm |F_P(hkl)|| - F_{Hcalc}/\Sigma_{hkl}||F_{PH}(hkl)| \pm |F_P(hkl)||$

The numbers in parentheses are given for the independent reflections.

Figure of merit value corresponds to an overall resolution shell of 19.88–2.5 Å.

superpositions were further refined with MAIN [40]. Structural figures were prepared with MOLSCRIPT [45], BOBSCRIPT [46], and RASTER3D [47]. Sequence alignments were drawn with ALSCRIPT [48].

Acknowledgments

This work was supported by the Deutsche Forschungsgemeinschaft, the Fonds der Chemischen Industrie, the Hans-Fischer-Gesellschaft e.V., and by NIH grant GM51469. We thank Gleb P. Bourenkov and Hans D. Bartunik for their assistance during the collection of the MAD data sets at DESY (Hamburg, Germany).

Received: April 11, 2002
Revised: July 10, 2002
Accepted: July 11, 2002

References

1. Bacher, A. (1991). Biosynthesis of flavins. In Chemistry and Biochemistry of Flavoenzymes, Volume I, F. Müller, ed. (Boca Raton, Florida: Chemical Rubber & Co.), pp. 215–259.
2. Bacher, A., Eberhardt, S., and Richter, G. (1996). Biosynthesis of riboflavin. In *Escherichia coli* and *Salmonella typhimurium*: Cellular and Molecular Biology, F.C. Neidhardt, ed. (Washington, DC: ASM Press), pp. 657–664.
3. Plaut, G.W.E., and Beach, R.L. (1976). Substrate specificity and stereospecific mode of action of riboflavin synthase. In Flavins and Flavoproteins, T.P. Singer, ed. (Amsterdam: Elsevier Scientific Publishing), pp. 737–746.
4. Wacker, H., Harvey, R.A., Winestock, C.H., and Plaut, G.W.E. (1964). 4-(1′-D-ribitylamino)-5-amino-2,6-dihydroxypyrimidine, the second product of the riboflavin synthetase reaction. J. Biol. Chem. *239*, 3493–3497.
5. Plaut, G.W.E., Beach, R.L., and Aogaichi, T. (1970). Studies on the mechanism of elimination of protons from the methyl group of 6,7-dimethyl-8-ribityllumazine of riboflavin synthase. Biochemistry *9*, 771–785.
6. Paterson, T., and Wood, H.C.S. (1969). Deuterium exchange of C7-methyl protons in 6,7-dimethyl-8-D-ribityllumazine, and studies of the mechanism of riboflavin biosynthesis. J. Chem. Soc. Commun. 290–291.
7. Beach, R.L., and Plaut, G.W.E. (1970). Stereospecificity of the enzyme synthesis of the o-xylene ring of riboflavin. J. Am. Chem. Soc. *92*, 2913–2916.
8. Illarionov, B., Eisenreich, W., and Bacher, A. (2001). A pentacyclic reaction intermediate of riboflavin synthase. Proc. Natl. Acad. Sci. USA *98*, 7224–7229.
9. Schott, K., Kellermann, J., Lottspeich, F., and Bacher, A. (1990). Riboflavin synthases of *Bacillus subtilis*. Purification and amino acid sequence of the α subunit. J. Biol. Chem. *265*, 4204–4209.
10. Liao, D.I., Wawrzak, Z., Calabrese, J.C., Viitanen, P., and Jordan, D.B. (2001). Crystal structure of riboflavin synthase. Structure *9*, 399–408.
11. Otto, M.K., and Bacher, A. (1981). Ligand-binding studies on light riboflavin synthase from *Bacillus subtilis*. Eur. J. Biochem. *115*, 511–517.
12. Cushman, M., Patrick, A., Bacher, A., and Scheuring, J. (1991). Synthesis of epimeric 6,7-bis(trifluoromethyl)-8-ribityllumazine hydrates. Stereoselective interaction with the light riboflavin synthase of *Bacillus subtilis*. J. Org. Chem. *56*, 4603–4608.
13. Cushman, M., Patel, H.H., Scheuring, J., and Bacher, A. (1992). ^{19}F NMR studies on the mechanism of riboflavin synthase. Synthesis of 6-(trifluoromethyl)-7-oxo-8-(D-ribityl)lumazine and 6-(trifluoromethyl)-7-methyl-8-(D-ribityl)lumazine. J. Org. Chem. *57*, 5630–5643.
14. Cushman, M., Mavandadi, F., Kugelbrey, K., and Bacher, A. (1998). Synthesis of 2,6-dioxo-(1*H*,3*H*)-9-N-ribitylpurine and 2,6-dioxo-(1*H*,3*H*)-8-aza-9-N-ribityl-purine as inhibitors of lumazine synthase and riboflavin synthase. Bioorg. Med. Chem. *6*, 409–415.
15. Harvey, R.A., and Plaut, G.W.E. (1966). Riboflavin synthetase from yeast. Properties of complexes of the enzyme with lumazine derivatives and riboflavin. J. Biol. Chem. *241*, 2120–2136.
16. Rowan, T., and Wood, H.C.S. (1963). The biosynthesis of riboflavin. Proc. Chem. Soc. (London), 21–22.
17. Rowan, T., and Wood, H.C.S. (1968). The biosynthesis of pteridines. Part V. The synthesis of riboflavin from pteridine precursors. J. Chem. Soc. C 452–458.
18. Beach, R.L., and Plaut, G.W.E. (1969). The formation of riboflavin from 6,7-dimethyl-8-ribityllumazine in acid media. Tetrahedron Lett. *40*, 3489–3492.
19. Bandrin, S.V., Beburov, M.I., Rabinovich, P.M., and Stepanov, A.L. (1979). Riboflavin auxotrophs of *Escherichia coli*. Genetika *15*, 2063–2065.
20. Wang, A. (1992). Isolation of vitamin B_2 auxotrophs and preliminary genetic mapping in *Salmonella typhimurium*. Yi Chuan Xue Bao *19*, 362–368.
21. Oltmanns, O., and Lingens, F. (1967). Isolation of riboflavin-deficient mutants of *Saccharomyces cerevisiae*. Z. Naturforsch. B *22*, 751–754.
22. Logvinenko, E.M., Shavlovskii, G.M., and Koltun, L.V. (1972). Preparation and properties of riboflavin-dependent mutants of *Pichia guilliermondii* Wickerham yeasts. Mikrobiologiia *41*, 1103–1104.
23. Bacher, A., Baur, R., Eggers, U., Harders, H.D., Otto, M.K., and Schnepple, H. (1980). Riboflavin synthases of *Bacillus subtilis*. Purification and properties. J. Biol. Chem. *255*, 632–637.
24. Eberhardt, S., Richter, G., Gimbel, W., Werner, T., and Bacher, A. (1996). Cloning, sequencing, mapping and hyperexpression of the ribC gene coding for riboflavin synthase of *Escherichia coli*. Eur. J. Biochem. *242*, 712–719.
25. Meining, W., Eberhardt, S., Bacher, A., and Ladenstein, R. (2001). Crystallization and preliminary crystallographic analysis of the recombinant N-terminal domain of riboflavin synthase. Acta Crystallogr. D *57*, 1296–1299.
26. Truffault, V., Coles, M., Diercks, T., Abelmann, K., Eberhardt, S., Lüttgen, H., Bacher, A., and Kessler, H. (2001). The solution structure of the N-terminal domain of riboflavin synthase. J. Mol. Biol. *309*, 949–960.
27. Gerhardt, S., Haase, I., Steinbacher, S., Kaiser, J.T., Cushman, M., Bacher, A., Huber, R., and Fischer, M. (2002). The structural basis of riboflavin binding to *Schizosaccharomyces pombe* 6,7-dimethyl-8-ribityllumazine synthase. J. Mol. Biol. *318*, 1317–1329.
28. Illarionov, B., Kemter, K., Eberhardt, S., Richter, G., Cushman, M., and Bacher, A. (2001). Riboflavin synthase of *Escherichia coli*. Effect of single amino acid substitutions on reaction rate and ligand binding properties. J. Biol. Chem. *276*, 11524–11530.
29. Cushman, M., Patel, H.H., Scheuring, J., and Bacher, A. (1993). ^{19}F-NMR studies of the mechanism of riboflavin synthase. Synthesis of 6-(trifluoromethyl)-8-(D-ribityl)lumazine and derivatives. J. Org. Chem. *58*, 4033–4042.
30. Plaut, G.W.E., and Beach, R.L. (1975). Interaction of riboflavin synthase with analogs of 6,7-dimethyl-8-ribityllumazine. In Chemistry and Biology of Pteridines, W. Pfleiderer, ed. (Berlin: de Gruyter), pp. 101–124.
31. Bown, D.H., Keller, P.J., Foss, H.G., Sedlmaier, H., and Bacher, A. (1986). Solution structures of 6,7-dimethyl-8-substituted lumazines. ^{13}C NMR evidence for intramolecular ether formation. J. Org. Chem. *51*, 2461–2467.
32. Beach, R.L., and Plaut, G.W.E. (1971). The synthesis, properties, and base-catalyzed interactions of 8-substituted 6,7-dimethyllumazines. J. Org. Chem. *36*, 3937–3943.
33. Paterson, T., and Wood, H.C.S. (1972). The biosynthesis of pteridines. Part VI. Studies of the mechanism of riboflavin biosynthesis. J. Chem. Soc. Perkin Trans. *I*, 1051–1056.
34. Al Hassan, S.S., Kulick, R.J., Livingstone, D.B., Suckling, C.J., Wood, H.C.S., Wrigglesworth, R., and Ferone, R. (1980). Specific enzyme inhibitors in vitamin biosynthesis. Part 3. The synthesis and inhibitory properties of some substrate and transition state analogs of riboflavin synthase. J. Chem. Soc. Perkin Trans. *I*, 2645–2656.
35. Leslie, A.G.W. (1998). MOSFLM 6.0 edit (Cambridge, UK).
36. Matthews, B.W. (1968). Solvent content of protein crystals. J. Mol. Biol. *33*, 491–497.
37. Otwinowski, Z. (1991). Maximum Likelihood Refinement of

Heavy-Atom Parameters, W. Wolf, P.R. Evans, and A.G.W. Leslie, eds. (Warrington, UK: SERC Daresbury Laboratory).
38. Otwinowski, Z., and Minor, W. (1997). Processing of X-ray diffraction data collected in oscillation mode. Methods Enzymol. *276*, 307–326.
39. CCP4 (Collaborative Computational Project 4) (1994). The CCP4 suite: programs for protein crystallography. Acta Crystallogr. D *50*, 760–763.
40. Turk, D. (1992). Development and usage of a macromolecular graphics program. PhD thesis, Technical University of Munich, Munich.
41. Brünger, A.T., Adams, P.D., Clore, G.M., DeLano, W.L., Gros, P., Grosse-Kunstleve, R.W., Jiang, J.-S., Kuszewski, J., Nilges, N., Pannu, N.S., et al. (1998). Crystallography and NMR system (CNS): a new software system for macromolecular structure determination. Acta Crystallogr. D *54*, 905–921.
42. Laskowski, R.A., MacArthur, M.W., Moss, D.S., and Thornton, J.M. (1993). PROCHECK: a program to check the stereochemical quality of protein structures. J. Appl. Crystallogr. *26*, 283–291.
43. Ramachandran, G.N., and Sasisekharan, V. (1968). Conformation of polypeptides and proteins. Adv. Protein Chem. *23*, 283–437.
44. Tripos, I. (1998). Sybyl Molecular Modelling System 6.7, St. Louis.
45. Kraulis, P.J. (1991). MOLSCRIPT: a program to produce both detailed and schematic plots of protein structures. J. Appl. Crystallogr. *24*, 946–950.
46. Esnouf, R.M. (1997). An extensively modified version of MolScript that includes greatly enhanced coloring capabilities. J. Mol. Graph. *15*, 112–113, 132–134.
47. Merritt, E.A., and Murphy, M.E.P. (1994). Raster3D version 2.0. A program for photorealistic molecular graphics. Acta Crystallogr. D *50*, 869–873.
48. Barton, G.J. (1993). ALSCRIPT a tool to format multiple sequences alignments. Protein Eng. *6*, 37–40.

Accession Numbers

The atomic coordinates have been deposited in the Protein Data Bank under ID code 1KZL (http://www.rcsb.org/pdb/).